Tyrosine 167: The Origin of the Radical Species Observed in the Reaction of Cytochrome c Oxidase with Hydrogen Peroxide in Paracoccus denitrificans †

ARTICLE *in* BIOCHEMISTRY · OCTOBER 2004

Impact Factor: 3.02 · DOI: 10.1021/bi048898i · Source: PubMed

Tyrosine 167: The Origin of the Radical Species Observed in the Reaction of Cytochrome *c* Oxidase with Hydrogen Peroxide in *Paracoccus denitrificans*†

Kerstin Budiman,‡ Aimo Kannt,‡ Sevdalina Lyubenova,§ Oliver-Matthias H. Richter,⊥ Bernd Ludwig,⊥ Hartmut Michel,‡ and Fraser MacMillan*,§

Institut für Physikalische & Theoretische Chemie and Center for Biomolecular Magnetic Resonance, Institut für Biochemie, Abteilung Molekulare Genetik, Johann Wolfgang Goethe-Universität Frankfurt, D-60439 Frankfurt am Main, Germany, and Max-Planck Institut für Biophysik, D-60439 Frankfurt am Main, Germany

Received May 28, 2004; Revised Manuscript Received July 9, 2004

ABSTRACT: Determination of the three-dimensional structure of cytochrome *c* oxidase, the terminal enzyme of the respiratory chain, from *Paracoccus denitrificans* offers the possibility of site-directed mutagenesis studies to investigate the relationship between the structure and the catalytic function of the enzyme. The mechanism of electron-coupled proton transfer is still, however, poorly understood. The P_M intermediate of the catalytic cycle is an oxoferryl state the generation of which requires one additional electron, which cannot be provided by the two metal centers. It is suggested that the missing electron is donated to this binuclear site by a tyrosine residue that forms a radical species, which can then be detected in both the P_M and $F^•$ intermediates of the catalytic cycle. One possibility to produce P_M and $F^•$ intermediates artificially in cytochrome *c* oxidase is the addition of hydrogen peroxide to the fully oxidized enzyme. Using electron paramagnetic resonance (EPR) spectroscopy, we assign a radical species detected in this reaction to a tyrosine residue. To address the question, which tyrosine residue is the origin of the radical species, several tyrosine variants of subunit I are investigated. These variants are characterized by their turnover rates, as well as using EPR and optical spectroscopy. From these experiments, it is concluded that the origin of the radical species appearing in P_M and $F^•$ intermediates produced with hydrogen peroxide is tyrosine 167. The significance of this finding for the catalytic function of the enzyme is discussed.

Cytochrome *c* oxidase (C*c*O;[1] for recent reviews, see *1*−*3*) is the terminal enzyme of the respiratory chain. Using cytochrome *c* as electron donor, it catalyses the reduction of oxygen to water and additionally pumps protons across the mitochondrial or bacterial membrane. This reaction contributes to the generation of a proton gradient across the membrane that is used by the ATP-synthase for the formation of ATP. The net reaction can be written as follows:

$$4\text{cyt } c^{2+} + O_2 + 8H_i^+ \rightarrow 4\text{cyt } c^{3+} + 2H_2O + 4H_o^+ \quad (1)$$

with H_i^+ denoting protons taken up from the inner phase (the bacterial cytoplasm or mitochondrial matrix) and H_o^+ referring to protons released into the outer phase (the periplasm or mitochondrial intermembrane space).

Although the structure (*4*−*6*) and function of C*c*O has been studied for many years, it is still a matter of debate how electron and proton transfer are coupled. During one turnover, electrons are transferred from cytochrome *c* initially to Cu_A, then further to heme *a*, and from there into the binuclear center made of heme a_3 and Cu_B where oxygen reduction takes place.

Substrate and vectorial protons are taken up from the cytoplasmic side of the membrane via two proton pathways (so-called D- and K-pathways), that have been identified by analysis of the protein structure and by site-directed mutagenesis experiments (*7*−*11*). The vectorial protons are transferred to the periplasmic side of the membrane via an as yet to be clearly identified proton exit pathway.

During one turnover of C*c*O several intermediates are formed that represent different redox states of the metal centers, and they have been characterized by several different spectroscopic approaches. A simplified scheme of the important features of the catalytic cycle relevant to this work is given in Figure 1. As shown in Figure 1A, the P_M state is generated after the binding of oxygen to the two-electron reduced binuclear site (R state) by electronic rearrangement on the microsecond time scale. After uptake of the third electron, the P_M state is converted to the F state. Then, after

† This work was supported by the Deutsche Forschungsgemeinschaft (Grant Sfb 472), the Center for Biomolecular Magnetic Resonance, the Max-Planck Gesellschaft, and Fonds der Chemischen Industrie.

* Corresponding author. Phone number: (+ 49 69) 798 29593. Fax number: (+ 49 69) 798 29404. E-mail: macmillan@epr.uni-frankfurt.de.

‡ Max-Planck Institut für Biophysik.

§ Institut für Physikalische & Theoretische Chemie and Center for Biomolecular Magnetic Resonance, Johann Wolfgang Goethe-Universität Frankfurt.

⊥ Institut für Biochemie, Abteilung Molekulare Genetik, Johann Wolfgang Goethe-Universität Frankfurt.

[1] Abbreviations: A_{iso}, isotropic hyperfine coupling; C*c*O, cytochrome *c* oxidase; cw, continuous wave; DPPH, (α,α′)-diphenyl-β-picrylhydrazyl; EDTA, ethylenediaminetetraacetic acid; EPR, electron paramagnetic resonance; ENDOR, electron nuclear double resonance; FTIR, Fourier transform infrared spectroscopy; hf, hyperfine; hfc's, hyperfine coupling constants; LM, *n*-dodecyl-β-D-maltoside; MES, 2-(*N*-morpholino)ethanesulfonic acid; o.d., outer diameter.

10.1021/bi048898i CCC: $27.50
Published on Web 08/21/2004

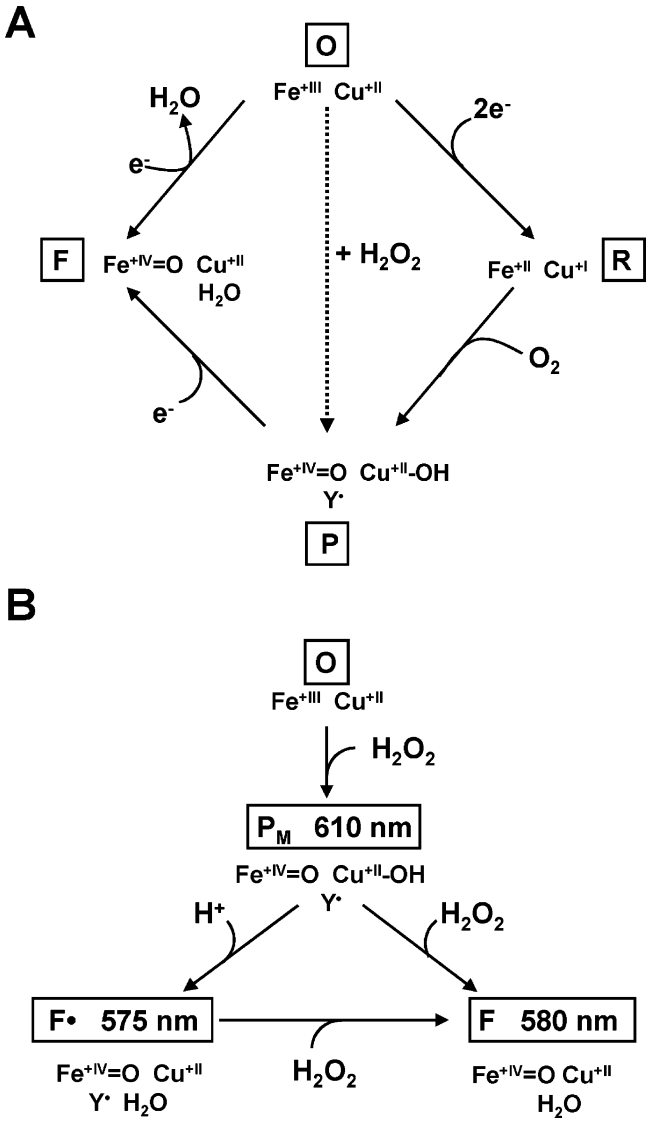

FIGURE 1: (A) Simplified reaction scheme of C*c*O excluding proton movements and (B) the specific reaction scheme of oxidized C*c*O and H_2O_2. For details, see the text.

insertion of the fourth electron to the binuclear site, the O state is regenerated.

The P_M state can be generated artificially by addition of stoichiometric amounts of hydrogen peroxide to the fully oxidized enzyme at high pH. The P_M state is characterized by a 610 nm maximum in the difference spectrum and by the appearance of a tyrosine radical species. If a second molecule of hydrogen peroxide is available, the P_M state can be converted to the F state, which shows a 580 nm maximum. When cytochrome *c* oxidase reacts with hydrogen peroxide at low pH, the P_M state is unstable, and the main product of the reaction is the $F^•$ state, which is characterized by a 575 nm maximum in the difference spectrum and the presence of the tyrosine radical. With an excess of hydrogen peroxide, the $F^•$ state is transferred to the F state.

In the present study, the generation of a tyrosine radical that is associated with the formation of P_M and $F^•$ states in C*c*O from *Paracoccus denitrificans* is investigated. Both the P_M and $F^•$ states can be generated either by addition of stoichiometric amounts of hydrogen peroxide to the fully oxidized enzyme or by aerobic incubation of the enzyme with carbon monoxide (*12*−*14*). Both these intermediate states are characterized optically by absorption band maxima at 610 or 575 nm, respectively, while the maximum for F lies at 580 nm (*15*).

The P_M state was initially thought to be a peroxy state (*16*), but it was later shown by a number of studies that the bound oxygen was already cleaved and that an oxoferryl state was present in the P_M intermediate (*15*, *17*, *18*). The formation of such an oxoferryl state, however, requires an additional electron, which is not thought to be provided by the metal centers (*15*, *19*). It has been suggested (*5*, *15*) that this electron could be donated by tyrosine 280 (*P. denitrificans* numbering system), which is cross-linked with histidine 276, a ligand to the Cu_B (*5*, *6*).

Electron paramagnetic resonance (EPR) spectroscopy was used to observe and to identify a radical signal, which is generated in the $F^•$ state after reaction of C*c*O from *P. denitrificans* with stoichiometric amounts of hydrogen peroxide at low pH (*20*). The observed radical species was unequivocally assigned to a tyrosine radical by applying EPR spectroscopy in combination with specific ^{2}H-labeling (*20*). When ring-deuterated tyrosine was incorporated into the enzyme, it was clearly demonstrated that the observed hyperfine (hf) interactions collapsed. In addition, it was shown that the hf interaction of the two C_β protons could be resolved allowing a determination of their dihedral angles (*20*). Based on a comparison with data available from the crystal structure (PDB entry 1QLE, *4*), the observed dihedral angle did not correspond to that of tyrosine 280.

EPR signals have also been observed for the catalytic intermediates of bovine C*c*O (*13*, *21*). In the bovine C*c*O, broad and narrow EPR signals were detected. The broad species could be detected in the $F^•$ state made either by treatment with excess hydrogen peroxide or after lowering the pH of a P_M state generated by the CO/O_2 method. If the $F^•$ state is generated with excess hydrogen peroxide, this broad radical is accompanied by an additional narrow EPR signal, which has been assigned to a porphyrin cation species (*21*, *22*). The broad EPR signal was attributed to a tryptophan radical species based on comparison of the observed cw electron nuclear double resonance (ENDOR) spectrum with that of cytochrome *c* peroxidase (*22*).

In this work, we further characterize the tyrosine radical species observed in *P. denitrificans* using several approaches. Multifrequency EPR (performed at 9, 34, and 285 GHz) is used to resolve the **g**-tensor of this species providing an insight into its electrostatic environment. The dihedral angles determined previously (*20*) are compared to those determined from the crystal structure model (PDB entry 1QLE, *4*) to provide an indication of which tyrosine residue may be responsible for this radical species and finally to ultimately clarify the origin of the radical, a series of conserved tyrosines are exchanged individually (Y35, Y167, Y267, Y280, Y328, and Y414) to phenylalanine (histidine in the case of Y280). These tyrosine residues are all within distances to the binuclear center where electron transfer is possible (<20 Å).

Both the formation of P_M and $F^•$ intermediates and the formation of a radical species are studied by optical absorption and EPR spectroscopy, respectively. From the results, we assign the origin of the radical associated with the hydrogen peroxide reaction to a specific tyrosine residue, and this finding is discussed with regard to the catalytic cycle.

MATERIALS AND METHODS

Site-Directed Mutagenesis. Site-directed mutagenesis in subunit I of C*c*O (cytochrome aa_3) from *P. denitrificans* was done according to the altered sites mutagenesis protocol (Promega, Heidelberg). The plasmid transfer into *P. denitrificans* was performed by triple mating using the *Paracoccus* strain AO1 and the *Escherichia coli* helper strain MM294 (*23*).

Enzyme Preparation. P. denitrificans wild-type and mutant cells were grown in succinate medium as described (*24*), except that the manganese content was decreased in the medium. C*c*O was isolated as described (*25*). Deuteration of tyrosine was performed as reported previously (*20*).

Activity Test. The turnover rates of the C*c*O variants were determined using horse heart cytochrome *c* (*26*). Cytochrome *c* was reduced with sodium dithionite, and excess of the reductant was removed with a Sephadex G-10 gel filtration column (Pharmacia). The cytochrome *c* concentration was determined spectroscopically with $\Delta\epsilon_{red-ox} = 18.7\ mM^{-1}\ cm^{-1}$. The oxidation of 50 μM cytochrome *c* (in 10 mM phosphate buffer, pH 7.0, 40 mM KCl, 0.05% LM) after addition of a suitable amount of oxidase was followed at 550 nm.

Optical Spectroscopy. Optical absorption spectroscopy was performed on an Agilent 8453 spectrophotometer and on a Perkin-Elmer Lambda 40 UV/vis spectrometer. For all experiments, 10 μM freshly isolated oxidized C*c*O (buffered in 1 mM Tris-HCl, pH 9 (8.6), 50 mM KCl, 0.05% LM) was used. In pH-shift experiments, the addition of 20 μL of 1 M MES−KOH, pH 6.0, to the sample resulted in a pH of 6. In all optical experiments, C*c*O and hydrogen peroxide were mixed in a 1:5 ratio.

Preparation of EPR Samples. For the EPR experiments, 200 μM C*c*O in the same buffer was used. The H_2O_2 concentration was determined spectroscopically ($\epsilon_{240\ nm} = 40\ M^{-1}\ cm^{-1}$), the concentration of the oxidized C*c*O with $\epsilon_{425\ nm} = 158\ mM^{-1}\ cm^{-1}$, and the yields of the P and F intermediates with $\epsilon_{607-630\ nm} = 11\ mM^{-1}\ cm^{-1}$ and $\epsilon_{580-630\ nm} = 5.3\ mM^{-1}\ cm^{-1}$.

The reaction was initiated by addition of one molar equivalent of H_2O_2 at 4 °C, and the samples were immediately transferred to the standard suprasil quartz EPR tubes (o.d. = 3 or 4 mm) and frozen in liquid nitrogen. Cyanide inhibited C*c*O was formed by incubation with potassium cyanide (5 mM) at 4 °C for several hours.

EPR Spectroscopy. X-Band continuous-wave (cw) and pulsed EPR spectra of the radical EPR signal were measured on a Bruker E580 ELEXSYS spectrometer. A standard dielectric ring Bruker EPR cavity (MD 5 W1) was used. The microwave frequency and magnetic field were measured using the Bruker internal frequency counter and field controller, respectively. Q-band EPR spectra were measured using a Bruker E-500 spectrometer with a standard Bruker resonator (ER 5106QT-W1). Both instruments were equipped with Oxford helium cryostats (ESR900 and CF935, respectively). High-field EPR (285 GHz) spectroscopy and spectral simulations were performed as described previously (*27*, *28*) using exactly the same sample as for X-band EPR measurements. Q-band spectra were simulated using a home-written simulation and fit program (*29*, *30*). The measured *g*-values were corrected for an offset against a known *g* standard (DPPH, $g = 2.003\ 51 \pm 0.000\ 02$). The isotropic coupling ($A_{iso} = {}^1/_3\{A_{xx} + A_{yy} + A_{zz}\}$) for the β-methylene protons can be calculated from the tensor components in Table 1. The isotropic hf-coupling of a β-proton is related to the neighboring carbon spin density, $\rho^{\pi}_{C_4}$, by the relationship

$$A_{iso}(H_\beta) = \rho^{\pi}_{C_4}(B' + B'' \cos^2 \theta) \qquad (2)$$

where B' and B'' are empirical constants, $\rho^{\pi}_{C_4}$ is the spin density distribution on C_4, and θ is the dihedral angle between the α-carbon p_z axis and the projected $C_\beta - H_\beta$ bond (*31*). Assuming a value of 5.0−5.8 mT for B'' (B' is negligible) as has been suggested for tyrosine radicals (*32*) and a spin density of $\rho^{\pi}_{C_4} = 0.38$ (*33*) the resulting dihedral angles ($\theta_{1,2}$) can be calculated.

Table 1: Experimental **g** Tensor (g_{ii}) and C_β-methylene Proton (A_{ii}) Hyperfine Couplings of the Observed Tyrosine Radical in Cytochrome *c* Oxidase of *Paracoccus denitrificans*

radical	tensor element	g_{ii}[b]	C_{β_1} A_{ii}[c]	C_{β_2} A_{ii}[c]
$Tyr^{\bullet}$	*xx*	2.0070(1)	13.0	19.0
	yy	2.0044(1)	11.0	19.6
	zz	2.0020(1)	11.0	19.0
	iso[a]	2.0048(1)	11.67	19.2

[a] Where $A_{iso} = {}^1/_3\{A_{xx} + A_{yy} + A_{zz}\}$ and $g_{iso} = {}^1/_3\{g_{xx} + g_{yy} + g_{zz}\}$. [b] From fits of the EPR powder spectrum (Figure 2C). Values in parentheses are estimated errors in the last digit calibrated against a sample of manganese (0.02%) doped magnesium oxide (*34*). [c] From fits of the EPR powder spectrum (Figure 2B); values in gauss.

RESULTS

In the presence of a stoichiometric amount of H_2O_2, an EPR signal is observed at $g = 2.0048$ with a partially resolved line shape at X-band (9.5 GHz) frequencies. This signal has previously been assigned to a tyrosine residue based on isotopic labeling (*20*). Both the *g*-factor and this resolved hyperfine structure are related to the spin density distribution and to the electrostatic environment of the radical.

Multifrequency EPR experiments performed at 9, 34, and 285 GHz reveal that the **g**-tensor of the radical (Figure 2A−C), the values of which are given in Table 1, can be clearly resolved at 285 GHz. All three turning points are broader than other protein-bound tyrosyl radicals and are typical of a tyrosine in an environment slightly more electropositive than Y_D (photosystem II) (*27*,*28*). The g_{xx} direction is especially broad, and the simulation indicates a Gaussian distribution in g_{xx} of ∼0.000 56 indicating an environment or the orientation of the radical that is highly disordered.

This **g**-tensor indicates that at X- and Q-band frequencies the overall width of the observed EPR spectrum is dominated by partially resolved hf-interactions. Such hyperfine structure is very sensitive especially to the orientation of the ring headgroup relative to the protein backbone (*33*,*35*). More specifically, the dominant features in the spectra arise from distinct hf-couplings of the β-methylene protons (β_1 and β_2) at C_β, which forms a bond with the tyrosine ring at position C_4 (see Figure 3 for labeling), while those of the α-protons at the phenol ring (C_3, C_5, C_2, and C_6) are smaller in magnitude, more anisotropic, and almost invariant.

With the use of fully deuterated tyrosine, it is possible to partially resolve the **g**-tensor even at 34 GHz (Figure 2A).

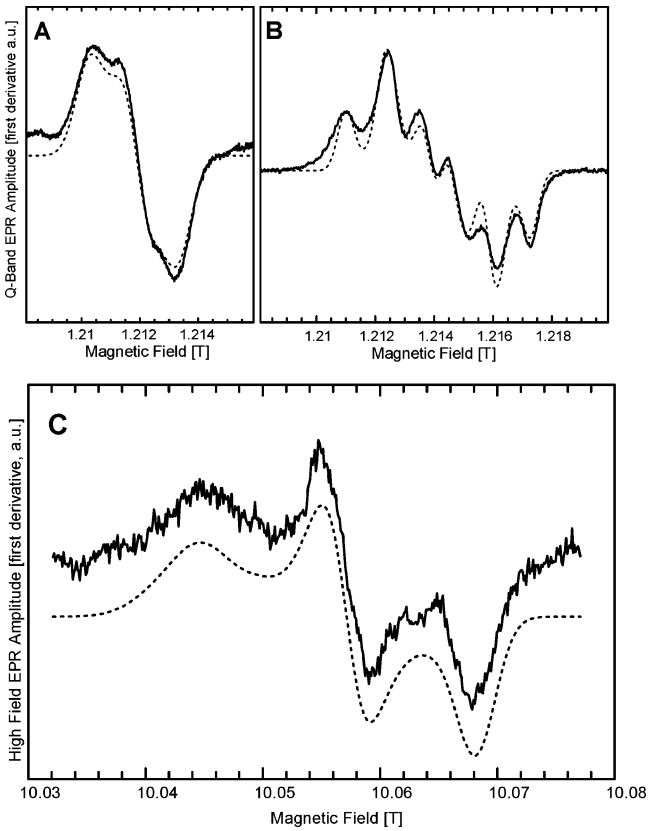

FIGURE 2: The EPR spectra (solid lines), together with spectral simulations (dotted lines), of wild-type C*c*O grown in Mn(II)-depleted medium treated with H_2O_2: (A) fully deuterated tyrosine recorded at 34 GHz; (B) ring-deuterated tyrosine recorded at 34 GHz; (C) fully protonated tyrosine recorded at 285 GHz. Experimental conditions for panels A and B were as follows: microwave power = 0.06 mW; field modulation = 12.5 kHz; amplitude = ±0.5 mT peak to peak; T = 80 K. Experimental conditions for panel C were the same as those for panels A and B, except microwave power nonsaturating and T = 10 K.

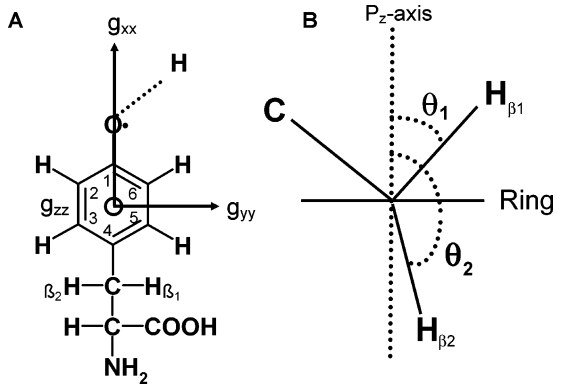

FIGURE 3: (A) Molecular structure, numbering scheme (inner numbers), and **g**-tensor axes system of the tyrosine radical and (B) edge-on view of tyrosine showing the side chain orientation together with the conformation of methylene protons, H_{β_1} and H_{β_2}. The respective dihedral angles are defined as the angle between the normal (the P_z orbital) to the tyrosine headgroup ring plane and the proton. The sign of the angle depends on whether it is rotated clockwise (positive) or anticlockwise with respect to the P_z orbital.

Spectral simulation provides the same **g**-tensor as that obtained from the measurement at 285 GHz. With the use of partially deuterated tyrosine, where only the ring protons have been deuterated, the hf-couplings from the methylene protons can be easily determined. Analysis of the Q-band EPR spectrum (Figure 2B) allows a direct determination of the dihedral angles (*31*, *32*). The resulting dihedral angles ($\theta_{1,2}$) are 140° ± 3° and 20° ± 5° (Table 2).

Table 2: Orientation of the Methylene Protons from the Crystal Structure and the Distances from the Carbonyl Oxygen of Tyrosine to the Iron of Heme a_3 and Cu_B in Cytochrome *c* Oxidase of *P. denitrificans* (PDB entry 1QLE *4*), Together with the Experimentally Determined Dihedral Angles as Defined in Figure 3

tyrosine	dihedral angle (deg)		distance [Å]	
residue	θ_1	θ_2	to Fe_{a_3}	to Cu_B
Y280	61.1	−57.8	5.3	5.0
Y328	58.7	186.7	10.7	9.3
Y167	20.8	138.1	13.6	10.7
Y407	−68.9	49.9	10.7	14.3
Y339	64.6	−55.9	15.9	12.7
Y267	−57.6	61.6	18.0	14.7
Y414	85.7	−33.8	14.8	19.3
Y406	85.5	−33.7	17.0	19.2
Y93	63.7	−54.9	24.0	28.2
Y35	−81.2	37.3	25.2	24.1
exptl results	20 ± 5	140 ± 3		

Table 3: Activities Including Yields of P_M and F States of Wild-Type Cytochrome *c* Oxidase of *P. denitrificans*, as Well as Selected Variants[a]

C*c*O	WT	Y35F	Y167F	Y267F	Y280H	Y328F	Y414F
activity [%]	100	45	62	7	<1	73	40
P state, pH 9 [%]	44	8	8	12	no	9	12
F state, pH 9	yes	no	no	no	no	no	no
F• state, pH 6 [%]	43	no	33	21	no	unstable	19
EPR signal	yes	yes	no	yes	yes	yes	yes

[a] Details are given in Materials and Methods.

To identify the origin of this radical species, a series of tyrosine variants were made and characterized. A list of the variants together with their activities including yields of P_M and F/F• states are given in Table 3. The turnover rates of all investigated variants are diminished compared to the wild-type enzyme. While the Y280H variant is completely inactive and Y267F is almost inactive, Y328F and Y167F showed quite high turnover rates with 73% and 62% of wild-type activity, respectively. It is difficult to understand why Y267F results in such a low activity. It may be of some structural importance or maybe also influences the proton exit pathway.

In each case, to prevent unspecific side reactions caused by an excess of hydrogen peroxide, work was performed using low hydrogen peroxide concentrations. These experiments reveal that formation of P_M, F• intermediates or both can be observed in all variants (except Y280H, see discussion). The P_M state can be produced by addition of low hydrogen peroxide concentrations to fully oxidized C*c*O at high pH. It can be characterized spectroscopically by a 610 nm maximum in the P_M minus O (oxidized) difference spectrum in the *Paracoccus* enzyme. At high pH, the transition from P_M to the F state can be seen in the steady state after several minutes. The F state can be distinguished from the P_M state by a 580 nm maximum in the F minus O difference spectrum. The experiments were performed with the wild-type enzyme and the tyrosine variants at pH 9 and a protein to hydrogen peroxide ratio of 1:5. The reaction was followed for 15 min. The maximum yields of P_M and F states were calculated from P_M minus O and F minus O difference spectra (Table 3).

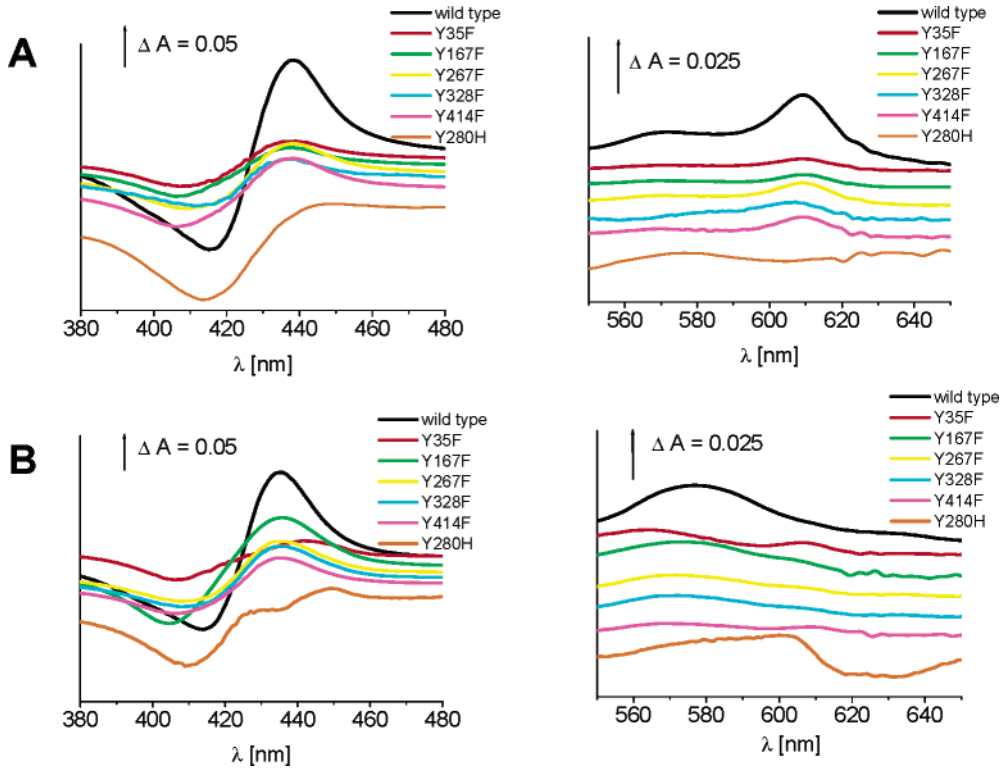

FIGURE 4: Panel A presents the optical difference spectra (P_M minus O) obtained from wild-type cytochrome *c* oxidase and the variants Y35F, Y167F, Y267F, Y328F, Y414F, and Y280H after the reaction with hydrogen peroxide at high pH. Experimental conditions were as follows: 10 μM of fully oxidized samples in 1 mM Tris-HCl, pH 9, 50 mM KCl, and 0.05% LM were mixed with 50 μM H_2O_2. Panel B presents optical difference spectra ($F^\bullet$ minus O) obtained from wild-type cytochrome *c* oxidase and the variants Y35F, Y167F, Y267F, Y328F, Y414F, and Y280H after a jump to acidic pH shortly before the reaction with hydrogen peroxide. Experimental conditions were as follows: 10 μM of fully oxidized samples in 1 mM Tris-HCl, pH 9, 50 mM KCl, and 0.05% LM were mixed with 50 μM MES-KOH, pH 6; after that, 50 μM H_2O_2 was added to the samples.

In Figure 4A, a comparison between the maximum yield of the P_M state in the wild-type enzyme and the tyrosine variants is shown. For the wild-type enzyme, the maximum yield of P_M is 44% referring to the concentration of the oxidized protein. In all tyrosine variants, the maximum yields, under the given experimental conditions, of the P_M state are much lower with values between 8% and 12%.

Only in the wild-type enzyme was the transition to the F state detectable after 15 min, while in all variants, the P_M state remained stable (except for Y280H where P_M is not formed under these conditions) in this time range (data not shown). Addition of the same amount of hydrogen peroxide to C*c*O after a pH-jump to pH 6 leads, after transient formation of a small amount of P_M, to the fast formation of the $F^\bullet$ state or to mixtures of $F^\bullet$ and F. The $F^\bullet$ minus O difference spectrum is very similar to the F minus O difference spectrum so that it is not possible to distinguish between the pure $F^\bullet$ state and mixtures that can be formed in the steady state.

Figure 4B shows the maximum yields of $F^\bullet$/F states when hydrogen peroxide (C*c*O to hydrogen peroxide ratio 1:5) is added after a pH jump to pH 6. The maximum $F^\bullet$/F yield of the wild-type enzyme is 43% referring to the concentration of the oxidized protein (Table 3). The variants Y167F, Y267F, and Y414F are able to generate $F^\bullet$/F states with a reduced yield compared to the wild-type enzyme. In the experiment performed with the variant Y35F, no 580 nm maximum could be detected; however, a small peak at 610 nm is present indicating that this variant forms a stable P_M state even at low pH. In the experiment with the variant Y328F, a maximum at 580 nm could be detected, but it was not stable over a longer time range. From these experiments, we conclude that all variants except Y280H are able to generate P_M and $F^\bullet$ states under these conditions (see Discussion).

For each of the variants, the EPR signal was generated in the same way as for wild-type enzyme, and the resulting spectra are shown in Figure 5. Radical signals were detected for the P_M state at high pH and for the $F^\bullet$ state after a pH jump to low pH for Y280H and for all other variants except of Y167F. From these results, we conclude that the radical associated with the hydrogen peroxide reaction does not arise from the residue Y280 but rather from Y167. Tyrosine 167 is located at a distance of about 10 Å from the binuclear center, which should be close enough to transfer an electron to the binuclear center (Figure 6).

In an attempt to characterize the appearance of this radical species, experiments were performed at several different pH values. This tyrosine radical in wild-type C*c*O can indeed be observed both at high (pH 9) and low pHs (pH 6), that is, in both the P_M and $F^\bullet$ states. In both cases, the partially resolved hyperfine structure is very similar (data not shown). In addition manual freeze−quench experiments reveal an identical spectral signature in the subsecond time scale after addition of hydrogen peroxide.

DISCUSSION

The results presented here provide direct evidence for a radical species generated in the reaction of C*c*O with H_2O_2

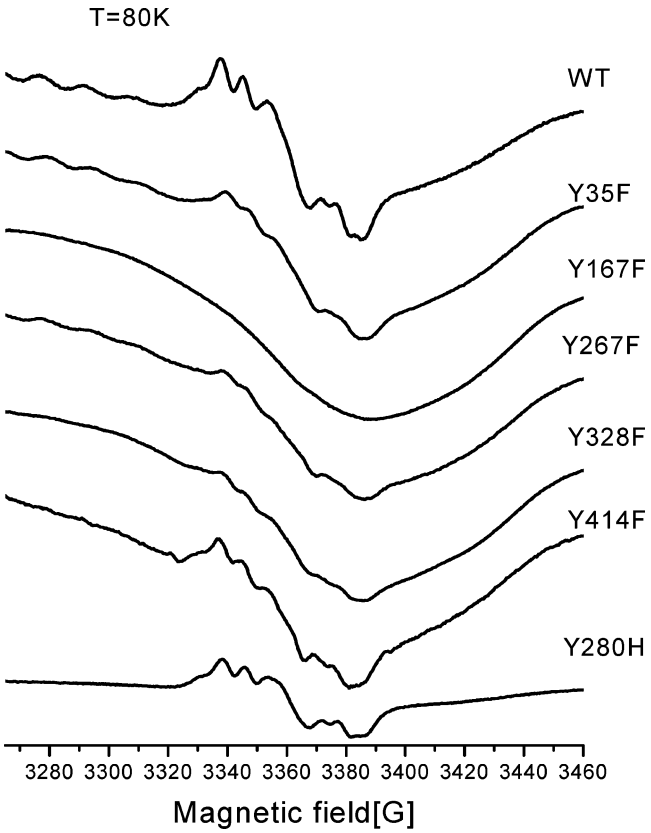

FIGURE 5: EPR spectra of the tyrosine radical after treatment of wild-type and variant C*c*O with H_2O_2. Experimental conditions were as follows: microwave power = 0.1 mW; field modulation = 12.5 kHz; amplitude = ±0.2 mT peak to peak; T = 80 K.

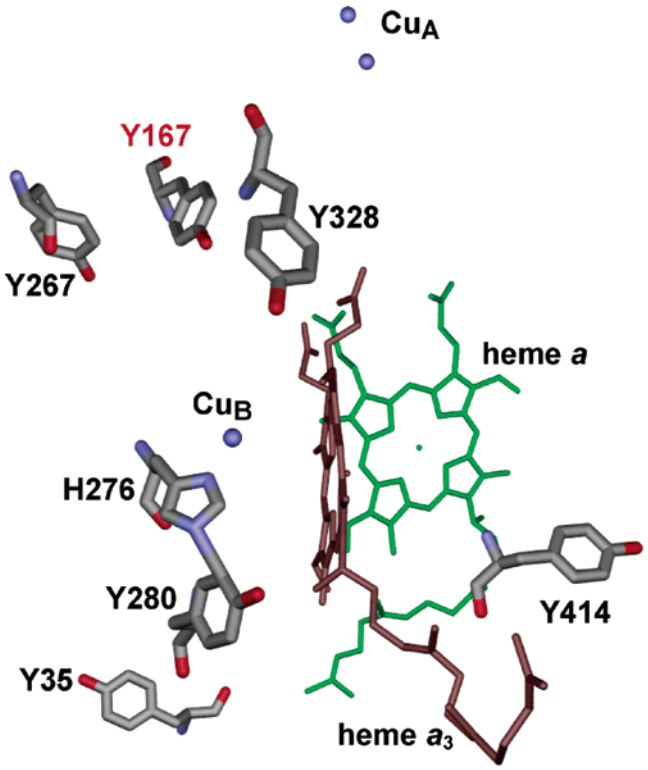

FIGURE 6: Section of the crystal structure showing the location of the main cofactors, as well as selected tyrosine residues and histidine 276, with respect to the binuclear center (data taken from PDB file 1QLE (*4*)).

in both P_M and F• states. High-field EPR gives *g*-values typical of tyrosine and not of any other amino acid radical (*30*, *36*). Further, based on the **g**-tensor values, the radical species is found in an electropositive environment, indicative of hydrogen bonding (*27*, *28*). Spectral analysis indicates that either the orientation of the radical is highly disordered or the hydrogen bonding is disordered. The clear resolution of the *β*-methylene proton couplings (Figure 2B) would suggest the latter. In addition, molecular dynamics simulations have also shown a disordered water structure in this region of the protein (*37*).

An important question is the yield of the observed radical and the conditions under which it is observed. In all EPR experiments performed in this work, a 1:1 stoichiometric amount of hydrogen peroxide is used, whereas in other studies with bovine C*c*O a large excess (10−500-fold) is applied (*13*, *14*, *21*). The yield of radical species formed in P_M and F• is about 20% relative to fully oxidized Cu_A. Thus the radical species occurs in ca. 50% of F• and P_M when compared to their respective yields (see Table 3).

As shown previously (*20*), it is confirmed that the radical generated in the reaction of C*c*O arises from a tyrosine residue. In addition a comparison of the dihedral angles determined previously from spectral simulation (*20*) and those analyzed from the crystal structure model (Figure 2 and Table 2) can be performed.

Assuming sp^3 hybridization, the resulting dihedral angle of the adjacent C_α atom (Figure 3) would be much closer to the ring plane than to the ring normal. A comparison with structural data and especially the dihedral angles (Table 2) suggests Y167 as the most likely candidate, provided that no reorientation of the radical species occurs upon formation.

Very recently, Svistunenko et al. (*38*) reported simulated EPR spectra for both the *P. denitrificans* and the bovine enzyme where they provide evidence that supports the possibility that in both enzymes a tyrosine residue is the origin of the radical formed in the reaction with hydrogen peroxide. They also ruled out that the signal could arise from residue Y280, because the rotational conformation of the phenolic ring was inconsistent with their spectral simulation. Instead they also suggested that Y167 could be the source of the radical because their simulation parameters were in agreement with the rotational conformation of this tyrosine. More importantly they also provide evidence that the radical species observed in the bovine system was also consistent with a tyrosine species based on spectral simulations of the published spectra (*21*) using identical parameters as those for the *P. denitrificans* system (*20*).

The yields of P, F•, and F intermediates that are detected by optical spectroscopy here for wild-type C*c*O from *P. denitrificans* are significantly lower than the yields observed in the bovine enzyme, but they are in the same range of that reported by Pinakoulaki et al. for the *Paracoccus* enzyme (*39*) and for *Rhodobacter sphaeroides* (*40*). The yields of P, F•, and F intermediates in the investigated tyrosine variants are much lower than that of the wild-type enzyme. This finding is in agreement with the lower yield of the EPR radical signal of the tyrosine variants. An important point to note is that with the exception of wild-type enzyme the addition of stoichiometric amounts of hydrogen peroxide to the enzyme does not result in the formation of P_M or F• (data not shown) with the time scale of 15 min. Another observa-

tion is the enzyme concentration dependence of the reaction of hydrogen peroxide. It is important to note that the optical experiments are performed at enzyme concentrations of ca. 10 μM, whereas the EPR samples have enzyme concentrations of 200 μM. It is estimated that the reaction rates of the enzyme increase nonlinearly with protein concentration (A. Kannt, unpublished data), so the reaction of Y280H with H_2O_2 (1:5) does not reveal the P_M or F• state optically but does reveal an EPR signal at much higher protein concentrations. Recent reports in the literature suggest that using a 500-fold molar excess of H_2O_2 does however result in the formation of P_M (*41*). Maybe either the large molar excess of the hydrogen peroxide or the high protein concentration result in the formation of P_M, which is not observed optically under stoichiometric (or 1:5 molar) ratio conditions.

In this study, only six variants within a 20 Å distance to the binuclear center have been studied. Three further tyrosines (Y407, Y339, and Y406) are also within a 20 Å radius of the binuclear center but are not conserved in the *bo*$_3$ quinol oxidase from *E. coli*. It has also been shown in this system that a radical species is formed after treatment with hydrogen peroxide with a very similar partially resolved hyperfine structure. Indeed after isotopic labeling with selectively deuterated tyrosine, this signal is also clearly assigned to a tyrosine residue (T. Ostermann, F. MacMillan, and H. Michel unpublished data); thus, variants at these positions were not studied.

The current site-directed mutagenesis studies demonstrate that a tyrosine radical species can be formed in the Y280H variant. This is a quite surprising result considering the debate in the literature with regard to the function of Y280.

Although the variant Y167F is able to generate P_M, F•, and F intermediates, it did not show a radical signal using EPR spectroscopy in these states (P, F•), even when the concentration of hydrogen peroxide was raised to a ratio of 1:5 or 1:10 (data not shown). Thus it appears that not Y280 but rather Y167 is the origin of this radical species that is observed in the reaction of C*c*O with hydrogen peroxide. Because the variant Y167F has a high turnover rate, major structural perturbations caused by the mutation that could destabilize the radical are unlikely. The role of the radical at this residue, which is positioned more than 13 Å away from the heme a_3 iron, remains unclear (Figure 6).

One explanation for the appearance of the radical in this position is to assume that the radical that occurs in the reaction of C*c*O with hydrogen peroxide is the radical of the steady state: Within the general scheme (Figure 1A), the electron postulated to arise from an amino acid and that results in cleavage of the oxygen−oxygen bond would be provided by Y280; the radical species is then eventually shifted to residue Y167, thus reaching a thermodynamically lower energy level.

An oxoferryl-cupric species with an additional protein radical has been proposed for both the P_M and F• states with the difference between the two states being a hydroxide ion bound to the Cu_B in P_M that is later protonated and thus a water in F• (*42*). This does not contradict the current finding that we observe a radical species at both pH 8 and pH 6 because the observed species (Y167) occurs at a distance of about 10−13 Å from the catalytic center.

While mutation of Y280 to either phenylalanine (not shown) or histidine yields an essentially inactive enzyme (*23*, *43*) with incomplete incorporation of Cu_B, a radical species is still observed in the variant Y280H after reaction with hydrogen peroxide. While this species can be inhibited with cyanide, it remains unclear in this variant how the radical species can be formed if one assumes the transient participation of Y280. This finding does not necessarily exclude a primary role for Y280 in the reaction cycle if one assumes an electronic relay network capable of providing the fourth electron, though not in a kinetically competent way.

ACKNOWLEDGMENT

Thomas Prisner (JWG University, Frankfurt, Germany) is acknowledged for his support. We are grateful to Hannelore Müller for excellent technical assistance (MPI, Frankfurt, Germany) and Ute Pfitzner (JWG University, Frankfurt, Germany) for the Y280H variant. Sun Un (CEA Saclay, France) is acknowledged for recording the high-field (285 GHz) EPR spectrum. Friedhelm Lendzian (TU Berlin, Germany) is acknowledged for his help with the EPR spectral simulations. The EPR division of Bruker (Rheinstetten, Germany) is acknowledged for the possibility to perform the Q-band EPR measurements.

REFERENCES

1. Schultz, B. E., and Chan, S. I. (2001) Structures and proton-pumping strategies of mitochondrial respiratory enzymes, *Annu. Rev. Biophys. Biomol. Struct. 30*, 23−65.
2. Richter, O.-M. H., and Ludwig, B. (2003) Cytochrome *c* oxidase − structure, function, and physiology of a redox-driven molecular machine, *Rev. Physiol. Biochem. Pharmacol. 147*, 47−74.
3. Brzezinski, P., and Larsson, G. (2003) Redox-driven proton-pumping by heme-copper oxidases, *Biochim. Biophys. Acta 1606*, 1−13.
4. Iwata, S., Ostermeier, C., Ludwig, B., and Michel, H. (1995) Structure at 2.8 Å resolution of cytochrome *c* oxidase from *Paracoccus denitrificans*, *Nature 376*, 660−669.
5. Ostermeier, C., Harrenga, A., Ermler, U., and Michel, H. (1997) Structure at 2.7 Å resolution of the *Paracoccus denitrificans* two-subunit cytochrome *c* oxidase complexed with an antibody Fv-fragment, *Proc. Natl. Acad. Sci. U.S.A. 94*, 10547−10553.
6. Tsukihara, T., Aoyama, H., Yamashita, E., Tomizaki, T., Yamaguchi, H., Shinzawa-Itoh, K., Nakashima, R., Yaono, R., and Yoshikawa, S. (1996) The whole structure of the 13-subunit oxidized cytochrome *c* oxidase at 2.8 Å, *Science 272*, 1136−1144.
7. Fetter, J. R., Quian J., Shapleigh, J., Thomas, J. W., Garcia-Horsman, J. A., Schmidt, E., Hosler, J., Babcock, G. T., Gennis, R. B., and Ferguson-Miller, S. (1995) Possible proton relay pathways in cytochrome *c* oxidase, *Proc. Natl. Acad. Sci. U.S.A. 92*, 1604−1608.
8. Brzezinski, P, and Ädelroth, P. (1998) Proton-controlled electron transfer in cytochrome *c* oxidase: functional role of the pathways through Glu 286 and Lys 362, *Acta Physiol. Scand. Suppl. 643*, 7−16.
9. Mills, D. A., and Ferguson-Miller, S. (1998) Proton uptake and release in cytochrome *c* oxidase: separate pathways in time and space? *Biochim. Biophys. Acta 1365*, 46−52.
10. Zaslavsky, D., and Gennis, R. B. (2000) Proton pumping by cytochrome oxidase: progress, problems and postulates, *Biochim. Biophys. Acta 1458*, 164−179.
11. Pfitzner, U., Hoffmeier, K., Harrenga, A., Kannt, A., Michel, H., Bamberg, E., Richter, O.-M. H., and Ludwig, B. (2000) Tracing the D-pathway in reconstituted site-directed mutants of cytochrome *c* oxidase from *Paracoccus denitrificans*, *Biochemistry 39*, 6756−6762.
12. Bickar, D., Bonaventura, J., and Bonaventura, C. (1982) Cytochrome *c* oxidase binding of hydrogen peroxide, *Biochemistry 21*, 2661−2666.
13. Fabian, M, and Palmer, G. (1995) The interaction of cytochrome oxidase with hydrogen peroxide: the relationship of compounds P and F, *Biochemistry 34*, 13802−13810.

14. Jünemann, S., Heathcote, P., and Rich, P. R. (2000) The reactions of hydrogen peroxide with bovine cytochrome *c* oxidase, *Biochim. Biophys. Acta 1456*, 56−66.
15. Proshlyakov, D. A., Pressler, M. A., and Babcock, G. T. (1998) Dioxygen activation and bond cleavage by mixed-valence cytochrome *c* oxidase, *Proc. Natl. Acad. Sci. U.S.A. 95*, 8020−8025.
16. Babcock, G. T., and Wikström, M. (1992) Oxygen activation and the conservation of energy in the cell, *Nature 356*, 301−309.
17. Proshlyakov, D. A., Ogura, T., Shinzawa-Itoh, K., and Kitagawa T. (1996) Resonance Raman/Absorption Characterization of Oxo Intermediates of Cytochrome *c* Oxidase Generated in its Reaction with Hydrogen Peroxide: pH and H_2O_2 Concentration Dependence, *Biochemistry 35*, 8580−8586.
18. Fabian, M., Wong, W. W., Gennis, R. B., and Palmer, G. (1999) Mass spectrometric determination of dioxygen bond splitting in the "peroxy" intermediate of cytochrome *c* oxidase, *Proc. Natl. Acad. Sci. U.S.A. 96*, 13114−13117.
19. Michel, H. (1999) Cytochrome *c* Oxidase: Catalytic Cycle and Mechanisms of Proton Pumping- A Discussion, *Biochemistry 38*, 15129−15140.
20. MacMillan, F., Kannt A., Behr, J., Prisner, T., and Michel, H. (1999) Direct Evidence for a Tyrosine Radical in the Reaction of Cytochrome *c* Oxidase with Hydrogen Peroxide, *Biochemistry 38*, 9179−9184.
21. Rigby, S. E., Jünemann, S., Rich, P. R., and Heathcote, P. (2000) Reaction of bovine cytochrome *c* oxidase with hydrogen peroxide produces a tryptophan cation radical and a porphyrin cation radical, *Biochemistry 39*, 5921−5928.
22. Rich, P. R., Rigby, S. E., and Heathcote, P. (2002) Radicals associated with the catalytic intermediates of bovine cytochrome *c* oxidase, *Biochim. Biophys. Acta 1554*, 137−146.
23. Pfitzner, U., Odenwald, A., Ostermann, T., Weingard, L., Ludwig, B., and Richter, O.-M. H. (1998) Cytochrome *c* oxidase (heme aa_3) from *Paracoccus denitrificans*: analysis of mutations in putative proton channels of subunit I, *J. Bioenerg. Biomembr. 30*, 89−97.
24. Ludwig, B. (1986) Cytochrome *c* oxidase from *Paracoccus denitrificans*, *Methods Enzymol. 126*, 153−159.
25. Kleymann, G., Ostermeier, C., Ludwig, B., Skerra, A., and Michel, H. (1995) Engineered Fv fragments as a tool for the one-step purification of integral multisubunit membrane protein complexes, *Biotechnology* (*N. Y.*) *13*, 155−160.
26. Witt, H., Malatesta, F., Nicoletti, F., Brunori, M., and Ludwig, B. (1998) Cytochrome-c-binding site on cytochrome oxidase in *Paracoccus denitrificans*, *Eur. J. Biochem. 251*, 367−373.
27. Un, S., Atta, M., Fontecave, M., and Rutherford, A. W. (1995) *g*-Values as a Probe of the Local Protein Environment: High Field EPR of Tyrosyl Radicals in Ribonucleotide Reductase and Photosystem II, *J. Am. Chem. Soc. 117*, 10713−10719.
28. Un, S., Gerez, C., Elleingand, E., and Fontecave, M. (2001) Sensitivity of Tyrosyl Radical *g*-Values to Changes in Protein Structure: A High Field EPR Study of Mutants of Ribonucleotide Reductase, *J. Am. Chem. Soc. 123*, 3048−3054.
29. Lendzian, F., Sahlin, M., MacMillan, F., Bittl, R., Fiege, R., Pötsch, S., Sjöberg, B.-M., Gräslund, A., Lubitz, W., and Lassmann, G. (1996) Electronic Structure of Neutral Tryptophan Radicals in Ribonucleotide Reductase Studied by EPR and ENDOR Spectroscopy, *J. Am. Chem. Soc. 118*, 8111−8120.
30. Bleifuss, G., Kolberg, M., Pötsch, S., Hofbauer, W., Bittl, R., Lubitz, W., Gräslund, A., Lassmann, G., and Lendzian, F. (2001) Tryptophan and Tyrosine Radicals in Ribonucleotide Reductase: A Comparative High-Field EPR Study at 94 GHz, *Biochemistry 40*, 15362−15368.
31. Stone, E. W., and Maki, A. H. (1962) Hindered internal rotation and ESR spectroscopy, *J. Chem. Phys. 37*, 1326−1333.
32. Fasanella, E. L., and Gordy, W. (1969) Electron spin resonance of an irradiated single crystal of L-tyrosine-HC, *Proc. Natl. Acad. Sci. U.S.A. 62*, 299−304.
33. Hoganson, C. W., Sahlin, M., Sjöberg, B.-M., and Babcock, G. T. (1996) Electron Magnetic Resonance of the Tyrosyl Radical in Ribonucleotide Reductase from *Escherichia coli*, *J. Am. Chem. Soc. 118*, 4672−4679.
34. Burghaus, O., Plato, M., Rohrer, M., Möbius, K., MacMillan, F., and Lubitz, W. (1993) 3-MM High-Field EPR on Semiquinone Radical Anions $Q^{\bullet-}$ Related to Photosynthesis and on the Primary Donor $P^{\bullet+}$ and Acceptor $Q_A^{\bullet-}$ in Reaction Centres of *Rhodobacter sphaeroides* R-26, *J. Phys. Chem. 97*, 7639−7647.
35. Bender, C. J., Sahlin, M., Babcock, G. T., Barry, B. A., Chandraseker, T. K., Salowe, S. P., Stubbe, J., Lindström, B., Petersson, L., Ehrenberg, A., and Sjöberg, B.-M. (1989) An ENDOR study of the tyrosyl free radical in ribonucleotide reductase from *Escherichia coli*, *J. Am. Chem. Soc. 111*, 8076−8083.
36. Duboc-Toia, C. Hassan, A. K., Mulliez, E., Ollagnier-de Choudens, S., Fontecave, M., Leutwein, C., and Heider, J. (2003) Very High-Field EPR Study of Glycyl Radical Enzymes, *J. Am. Chem. Soc. 125*, 38−39.
37. Olkhova, E., Hutter, C., Lill, M. A., Helms, V., and Michel, H. (2004) Dynamic Water Networks in Cytochrome *c* Oxidase from *Paracoccus denitrificans* Investigated by Molecular Dynamics Simulations, *Biophys. J. 86*, 1873−1889.
38. Svistunenko, D. A., Wilson, M. T., and Cooper, C. E. (2004) Tryptophan or tyrosine? On the nature of the amino acid radical formed following hydrogen peroxide treatment of cytochrome *c* oxidase, *Biochim. Biophys. Acta 1655*, 372−380.
39. Pinakoulaki, E., Pfitzner, U., Ludwig, B., and Varotsis C. (2002) The Role of the Cross-link His-Tyr in the Functional Properties of the Binuclear Center in Cytochrome *c* Oxidase, *J. Biol. Chem. 277*, 13563−13568.
40. Pecoraro, C., Gennis, R. B., Vygodina, T. V., and Konstantinov, A. A. (2001) Role of the K−Channel in the pH-Dependence of the Reaction of Cytochrome *c* Oxidase with Hydrogen Peroxide, *Biochemistry 40*, 9695−9708.
41. Pinakoulaki, E., Pfitzner, U., Ludwig, B., and Varotsis, C. (2003) Direct Detection of Fe(IV)═O Intermediates in the Cytochrome aa_3 oxidase from *Paracoccus denitrificans*/H_2O_2 Reaction, *J. Biol. Chem. 278*, 18761−18766.
42. Michel, H. (1998) The mechanism of proton pumping by cytochrome *c* oxidase, *Proc. Natl. Acad. Sci. U.S.A. 95*, 12819−12824.
43. Das, T. K., Pecoraro, C. Tomson, F. L., Gennis, R. B., and Rousseau, D. L. (1998) The posttranslational modification in cytochrome *c* oxidase is required to establish a functional environment of the catalytic site, *Biochemistry 37*, 14471−14476.

BI048898I